2018 26th Mediterranean Conference on Control and Automation (MED)
Zadar, Croatia, June 19-22, 2018

Optimization-based PV/PI Design for a DC-Motor System with Delayed Feedback

S. Mert Özer[1] Senem Yıldız[2] Altuğ İftar[3]

Abstract— **Proportional velocity (PV) and proportional integral (PI) controllers are designed to regulate the angular position and angular velocity, respectively, of a DC motor system with a pointwise time-delay in the feedback loop. Because of the time-delay, the system is described by delay-differential equations which have infinitely many modes that can not be assigned by using classical pole placement methods. The proposed method is based on minimizing the real part of the rightmost closed-loop mode, i.e., spectral abscissa, as a function of the controller parameters. The effectiveness of the method is illustrated by simulations and real-time experiments.**

I. Introduction

Proportional-integral (PI), proportional-derivative (PD), and proportional-integral-derivative (PID) controllers are the most popular controllers used in the industrial applications [1]. However, even though a controller is designed properly for the delay-free system, a certain amount of time-delay in the feedback loop may destroy time-domain performance or even cause instability [2]. Unlike the delay-free systems, time-delay systems have infinitely many modes [3]. Since the assignment of infinitely many modes is infeasible, the well-known pole placement methods can not be used for such systems. The best known method to compensate for a single input or output time-delay in a single-input single-output system is perhaps the Smith predictor [4]. Smith predictor, however, is not robust to variations in the time-delay or the plant transfer function and may produce an unstable response, especially when the open-loop plant is unstable. Although modifications to the Smith predictor have so far been proposed (e.g., [5], [6]), alternative methods, such as operator-theoretic [7] and Lyapunov-based [8] methods have also become available. Various methods, such as those based on the Lambert W function [9], [10], have also been proposed to design PID controllers. Eigenvalue-based approaches [3] have also proved to be useful to design controllers for linear time-invariant (LTI) time-delay systems. One such approach is the *non-smooth optimization*-based design approach, proposed in [11]. In this approach, closed-loop stability is achieved through minimizing the real part of the rightmost closed-loop mode, i.e., *spectral abscissa*, as a function of the controller parameters. This method relies on the fact that the modes move continuously with respect to small changes in the controller parameters. This method has successfully been applied to various control problems (e.g., [12]–[15]). A software package [16] have also been developed recently to apply this method.

In the present paper, we apply the non-smooth optimization-based approach to design proportional velocity (PV) and proportional integral (PI) controllers to regulate the angular position and angular velocity, respectively, of a DC motor system with a pointwise time-delay in the feedback loop. First, in Section II, we present the spectral properties of retarded time-delay systems to form the necessary background. In Section III, the time-domain performance and stability characteristics of the DC-motor control system with a time-delay in the feedback loop are analyzed. The proposed design approach is introduced in Section IV and PV and PI controllers are designed. The performance of the designed controllers are illustrated by both simulations and real-time experiments.

Throughout the paper, $\mathbb{R}$ and $\mathbb{C}$ respectively denote the sets of real and complex numbers. For $s \in \mathbb{C}$, $\mathrm{Re}(s)$ denotes the real part of s. For $\varepsilon \in \mathbb{R}$, $\mathbb{C}_\varepsilon^+ := \{s \in \mathbb{C} \mid \mathrm{Re}(s) \geq \varepsilon\}$. For a non-negative integer k, $\mathbb{R}^k$ and $\mathbb{C}^k$ respectively denote the spaces of k-dimensional real and complex vectors. I denotes the identity matrix of appropriate dimensions. Also, $\det(\cdot)$, $(\cdot)^T$, and $(\cdot)^H$ respectively denote the determinant, the transpose, and the complex-conjugate transpose of $(\cdot)$. Finally, j denotes the imaginary unit.

II. Spectral Properties of Delay-Differential Equations

In this section, to form the necessary background, we present the spectral properties of retarded time-delay systems. A LTI retarded time-delay system with a pointwise time-delay, $h > 0$, can be described by the (matrix) delay-differential equation (DDE):

$$\dot{x}(t) = A_0 x(t) + A_1 x(t-h) \tag{1}$$

where $x(t) \in \mathbb{R}^n$ is the state vector at time t. For any given $\varepsilon \in \mathbb{R}$, the set of ε-*modes* of (1) is defined as $\Omega_\varepsilon = \{s \in \mathbb{C}_\varepsilon^+ \mid \det(\phi(s)) = 0\}$ where

$$\phi(s) := sI - A_0 - A_1 e^{-hs}, \tag{2}$$

is the characteristic matrix of (1). Any $s^* \in \Omega_\varepsilon$ is said to be an ε-mode of the system (1). Furthermore, an ε-mode s^* is said to be *simple*, if $\frac{d}{ds}(\det(\phi(s)))|_{s=s^*} \neq 0$ and is said to be *multiple*, with *multiplicity* $r > 1$, if $\frac{d^k}{ds^k}(\det(\phi(s)))|_{s=s^*} = 0$, for $k = 1, \ldots, r-1$, and $\frac{d^r}{ds^r}(\det(\phi(s)))|_{s=s^*} \neq 0$.

It is well known that the system defined by (1) is stable if and only if $\Omega_0 = \emptyset$ [3]. This condition can equivalently be

This work is supported by the Scientific and Technical Research Council of Turkey (TÜBİTAK) under grant number 115E379. The authors are with the Department of Electrical and Electronics Engineering, Anadolu University, Eskişehir, Turkey.
{[1] smozer , [2] senemyildiz , [3] aiftar} @anadolu.edu.tr

stated in terms of the *spectral abscissa*, defined as

$$c := \sup\{\mathrm{Re}(s) \mid \det(\phi(s)) = 0\} \ . \tag{3}$$

Accordingly, (1) is *stable* if and only if $c < 0$. Therefore, to determine the stability of (1), Ω_ε must be obtained for some $\varepsilon < 0$. Although, a time-delay system has infinitely many modes, in general, since (1) is retarded, there are always a finite number of modes in $\mathbb{C}_\varepsilon^+$ for any $\varepsilon \in \mathbb{R}$ [17]. In this case, for any $\varepsilon \in \mathbb{R}$, the ε-modes of (1) can be calculated by the spectral method of [18]. Note that, since Ω_ε is always a finite set, the *supremum* in (3) can be reduced to a *maximum*.

Since c is a continuous function of h, it follows that a stable system can become unstable only when at least one mode crosses imaginary axis as h changes [3]. In this sense, a *delay margin* can be defined as the minimum additional time-delay that cause a stable system to become unstable.

III. DC-motor Modeling and Control

As an experimental platform, we use SRV-02 rotary based DC servo-motor system of Quanser [19]. The platform consists of a mechanical unit composed of a load shaft, a data acquisition device, a power amplifier, an actuator that consists of a DC servo-motor driven by a voltage amplifier, and sensors, an encoder and a tachometer, which measure the angular position and angular speed of the load shaft, respectively. The system is controlled using Matlab/Simulink integrated with QUARC software which allows implementing controllers designed in the following sections.

In the present study, we consider position and speed control of the DC-motor system when there exist a pointwise time-delay in the feedback loop. For this, the sensor outputs are exposed to an artificial time-delay which can be readily introduced in Simulink.

A. Position Control

The transfer function from the input motor voltage to the load shaft can be described as:

$$P(s) := \frac{\theta(s)}{V_m(s)} = \frac{K}{s(\tau s+1)} \tag{4}$$

where θ is the load shaft angle and V_m is the input voltage. The system gain K and the time constant τ are

$$\tau = 0.0254[s] \quad K = 1.53[\frac{rad}{V \times s}] \tag{5}$$

according to the system parameters given in [19]. In order to regulate the shaft angle, a proportional-velocity (PV) controller is used. The control structure is in the form of

$$V_m(t) = k_p(\theta_d(t) - \theta(t-h)) - k_v\dot{\theta}(t-h) \ , \tag{6}$$

which corresponds to a proportional plus negative velocity feedback, where θ_d is the reference for the shaft angle, k_v is the velocity feedback gain, and k_p is the proportional control gain. Furthermore, there exists a pointwise time-delay, denoted as h, in the feedback loop which renders $V_m(t)$

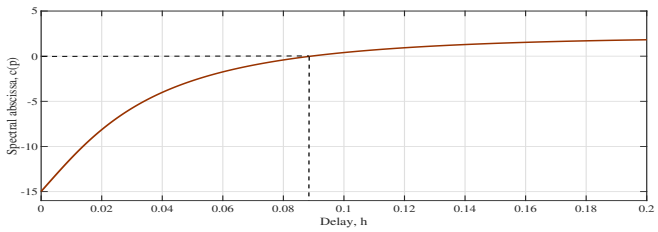

Fig. 1. Spectral abscissa of (8) with (9) for increasing values of delay.

to be a function of delayed output variables. The closed-loop transfer function of the system under the control (6) becomes

$$\frac{\theta(s)}{\theta_d(s)} = \frac{Kk_p}{\tau s^2 + s + Kk_v s e^{-hs} + Kk_p e^{-hs}} \ . \tag{7}$$

The corresponding DDE is

$$\dot{x}(t) = \begin{bmatrix} 0 & 1 \\ 0 & -\frac{1}{\tau} \end{bmatrix} x(t) + \begin{bmatrix} 0 & 0 \\ -\frac{Kk_p}{\tau} & -\frac{Kk_v}{\tau} \end{bmatrix} x(t-h) + \begin{bmatrix} 0 \\ \frac{Kk_p}{\tau} \end{bmatrix} \theta_d(t) \tag{8}$$

where $x(t) := \begin{bmatrix} \theta(t) & \dot{\theta}(t) \end{bmatrix}^T$ is the state vector at time t.

When we assume that $h = 0$, i.e., there is no delay, the DDE given in (8) becomes an ordinary differential equation (ODE). In this case, the controller gains can be determined by assigning the desired closed-loop poles $\lambda_d = -\omega_n\zeta \pm j\omega_n\sqrt{1-\zeta^2}$. to meet required time-domain specifications. In [19], a peak time less than or equal to 0.2s and an overshoot less than or equal to 5% is required. These time-domain specifications correspond to a desired damping ratio $\zeta = 0.690$ and a desired natural frequency $\omega_n = 21.7 rad/s$. According to that, the controller gains

$$k_p = 7.82[\frac{V}{rad}] \qquad k_v = -0.157[\frac{V \times s}{rad}] \ , \tag{9}$$

which assign $\lambda_d = -14.97 \pm 15.7j$, can be directly calculated by the formulas $k_p = \frac{\omega_n^2 \tau}{K}$ and $k_v = \frac{2\zeta\omega_n\tau - 1}{K}$. Since the autonomous part of (8) is in the form of (1), the spectral properties of (8) can be analyzed as for (1). As shown in Fig. 1, the delay margin of (8) with (9) is determined as about 0.085s. Furthermore, it is illustrated in Fig. 2 that the

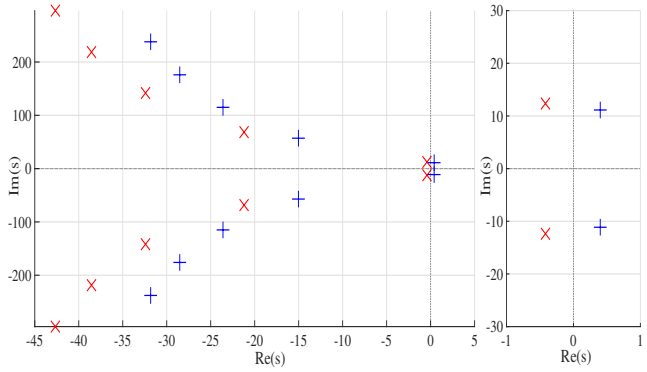

Fig. 2. -45-modes of (8) with (9) when $h = 0.08$ (red "x") and when $h = 0.1$ (blue "+").

rightmost modes cross the imaginary axis when the delay is increased from 0.08 to 0.1 seconds. Accordingly, as seen in the Fig. 3, the closed-loop system shows unsatisfactory

performance when $h = 0.08$, and shows unstable behavior when $h = 0.1$.

B. Speed Control

The transfer function from the input motor voltage to the load shaft angular speed can be described as:

$$P(s) := \frac{\Omega(s)}{V_m(s)} = \frac{K}{\tau s + 1} \tag{10}$$

where Ω is the angular speed of the load shaft, V_m is the input voltage, and K and τ are as in (4). In order to regulate the shaft speed, we use a proportional-integral (PI) controller in the form of

$$V_m(t) = k_p(\omega_d(t) - \omega(t-h)) + v(t)\,, \tag{11}$$

where ω_d is the reference for the shaft speed, k_p is the proportional control gain, and

$$v(t) := k_i \int_0^t (\omega_d(\sigma) - \omega(\sigma - h))\, d\sigma \tag{12}$$

is the output of the integrator, where k_i is the integral gain.

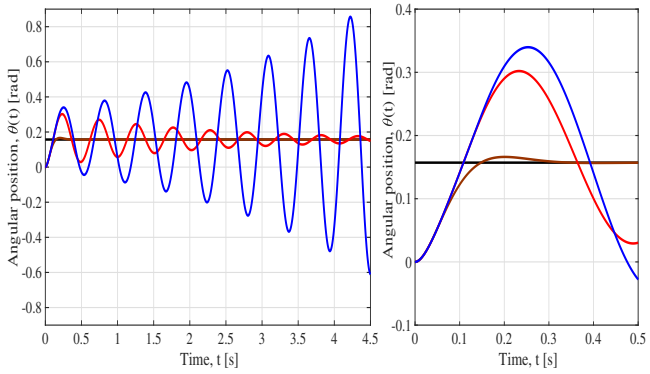

Fig. 3. Simulated response of the angular position with the gains $k_p = 7.82$ and $k_v = -0.157$. The brown, red, and blue curves correspond to the response when $h = 0$, $h = 0.08$, and $h = 0.1$, respectively, and the black line is the reference.

Because of the delay in the feedback loop, $V_m(t)$ is a function of delayed angular speed. The closed-loop transfer function under the control (11) is

$$\frac{\Omega(s)}{\Omega_d(s)} = \frac{K(k_p s + k_i)}{\tau s^2 + s + K k_p s e^{-hs} + K k_i e^{-hs}}\,. \tag{13}$$

The corresponding DDE is

$$\dot{x}(t) = \begin{bmatrix} -\frac{1}{\tau} & \frac{K}{\tau} \\ 0 & 0 \end{bmatrix} x(t) + \begin{bmatrix} -\frac{K k_p}{\tau} & 0 \\ -k_i & 0 \end{bmatrix} x(t-h) + \begin{bmatrix} \frac{K k_p}{\tau} \\ k_i \end{bmatrix} \omega_d(t) \tag{14}$$

where $x(t) := [\omega(t)\ v(t)]^T$ is the state vector at time t.

As in the position control, we first consider the case of $h = 0$. In [19], it is required that a peak time less than or equal to $0.05s$ and an overshoot less than or equal to 5%, which correspond to a $\zeta = 0.690$ and $\omega_n = 86.7 rad/s$ is desired. Respectively, the desired closed-loop system modes are $\lambda_d = -59.82 \pm 62.75$j. The controller gains

$$k_p = 1.34[\frac{V}{rad/s}] \qquad k_i = 124.9[\frac{V}{rad}] \tag{15}$$

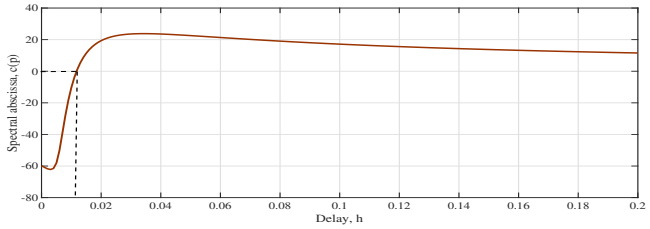

Fig. 4. Spectral abscissa of (14) with (15) for increasing values of delay.

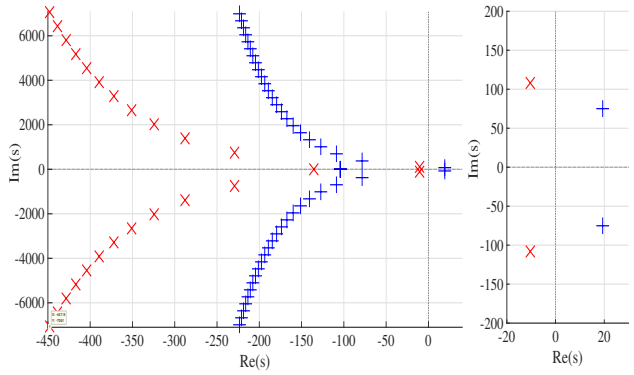

Fig. 5. -450-modes of (14) with (15) when $h = 0.01$ (red "x") and when $h = 0.02$ (blue "+").

can be calculated according to the formulas $k_p = \frac{2\zeta\omega_n\tau - 1}{K}$ and $k_i = \frac{\omega_n^2 \tau}{K}$.

As shown in Fig. 4, the delay margin of (14) with (15) is determined as about $0.012s$. Furthermore, it is evidenced by Fig. 5 that the rightmost modes cross the imaginary axis when the delay is increased from 0.01 to 0.02. Therefore, once again we encounter that a certain amount of delay makes the closed-loop system unstable. Accordingly, as seen in the Fig. 6, the closed-loop system shows unsatisfactory performance when $h = 0.01$, and shows unstable behavior when $h = 0.02$.

C. Measurement of the Angular Speed

Both PV and PI control structures require angular speed of the load shaft. Although the angular speed can be measured directly by the tachometer, these measurements are susceptible to noise. Another alternative is to take the derivative

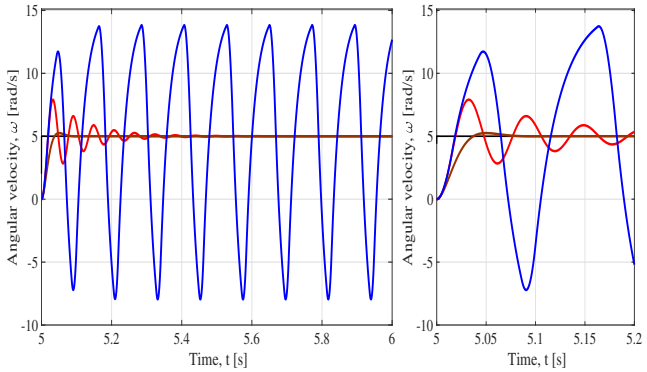

Fig. 6. Simulated response of the angular speed with (15). The brown, red, and blue curves correspond to the response when $h = 0$, $h = 0.01$, and $h = 0.02$, respectively, and the black line is the reference.

of the angular position measurement, obtained from the encoder. However, it is generally not advised to take the direct derivative of a measured signal, since it may contain high frequency noise components. Therefore, here we obtain the derivative by using the high-pass filter, given in [19]. In our experiments, we use both methods to measure the angular speed and present the results for both cases below.

IV. Controller Design

According to the delay margins determined in the previous section, neglecting the delay in the controller design phase may lead to instability if there exist significant amount of delay. Therefore, in this section, we aim to find controller parameters in (6) and (11) when $h \neq 0$.

Since (1) has an infinite number of modes, full assignment of those modes is not possible. However, as indicated in Section II, Ω_ε is a finite set for any $\varepsilon \in \mathbb{R}$. Furthermore, the location of the ε-modes is a continuous function of the controller parameters. Relying on that, the ε-modes of the system can be moved by tunning the controller parameters iteratively.

First, let us define the vector $p \in \mathbb{R}^2$ which contains the controller parameters in (8) or (14) (i.e., $p = \begin{bmatrix} k_p & k_v \end{bmatrix}$ or $p = \begin{bmatrix} k_p & k_i \end{bmatrix}$, respectively). Since the controller parameters are involved in the delayed part of (8) and (14), the matrix A_1 in (1) and, thus, the spectral abscissa c depend on p. Therefore, from now on, we will show this dependence explicitly as $A_1(p)$ and $c(p)$.

In order to achieve a stable closed-loop system, the stabilization problem can be reduced to minimization of the spectral abscissa of the closed-loop system over the parameters of the controller. As a result, the stabilizing controller parameters can be found by solving

$$\min_{p \in \mathbb{R}^2} c(p) \,. \tag{16}$$

Then, a stabilizing controller is obtained if $c(p) < 0$ is achieved.

As indicated in [11], spectral abscissa is a non-convex and nonsmooth function. Although (16) can be solved by using a gradient based algorithm, standard gradient based algorithms may fail because of the non-smoothness of the objective function. Therefore, we use specialized algorithms, namely the *gradient sampling algorithm* of [20] and the *BFGS method* of [21]. The optimization algorithms have already been implemented in a MATLAB-based software named as HANSO [22]. HANSO requires only a user-provided routine which returns the function value and the gradient vector at the current iterate. Therefore, we need to evaluate the spectral abscissa and the corresponding gradient.

The spectral abscissa is simply the real part of the (one of the) rightmost mode(s). To find the rightmost mode(s), we need to find the ε-modes for an appropriate ε. These, in turn, can be computed by the method of [18], which utilizes a spectral discretization approach and Newton's methods. Once the ε-modes are obtained, by definition (3), spectral abscissa can be obtained by taking the real part of the (one of the) rightmost mode(s).

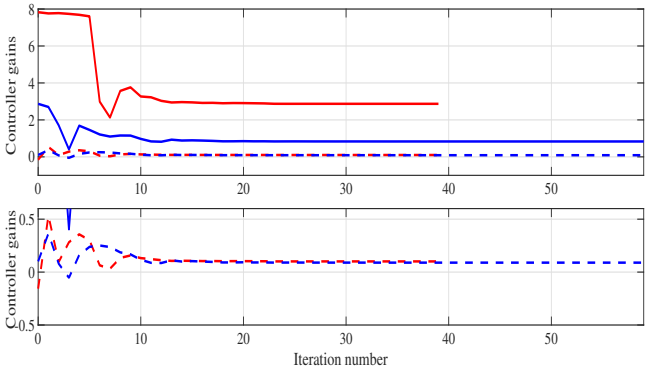

Fig. 7. Tunning of controller gains during the course of the optimization process. The straight lines are for k_p values; the dashed lines are for k_v values. Red color is used for case A-1; blue color is used for case A-2.

To find the gradient of the spectral abscissa, we need to calculate the partial derivatives of the (one of the) rightmost mode(s) with respect to the controller parameters. Let s^* be the (one of the) rightmost mode(s) when $p = p^*$ and p_j be the j^{th} element of p. Then, assuming a simple s^*, we can obtain (see [23])

$$\frac{\partial s^*}{\partial p_j}(p^*) = \frac{u^H \left(\frac{\partial A_1(p)}{\partial p_j}\Big|_{p=p^*} e^{-hs^*} \right) v}{u^H \left(I + A_1(p^*) h e^{-hs^*} \right) v} \,, \tag{17}$$

where $u, v \in \mathbb{C}^n$ are non-zero vectors satisfying $u^H \phi(s^*; p^*) = 0$ and $\phi(s^*; p^*) v = 0$, where $\phi(s; p)$ is the characteristic matrix defined in (2). Thus,

$$\frac{\partial c}{\partial p_j}(p^*) = \mathrm{Re}\left(\frac{\partial s^*}{\partial p_j}(p^*) \right) \tag{18}$$

and the gradient of c with respect to p at $p = p^*$ is

$$\nabla c(p^*) = \begin{bmatrix} \frac{\partial c}{\partial p_1}(p^*) & \frac{\partial c}{\partial p_2}(p^*) \end{bmatrix} . \tag{19}$$

It should be noted that (17) is valid only when s^* is a simple mode. If the rightmost mode, however, is a multiple mode with multiplicity $r > 1$, then, assuming that it is a controllable and observable mode [24], it can easily be separated into r simple modes by perturbing the controller parameters [23].

A. Position Control ($h \neq 0$)

In order to design a controller for (8), we will solve (16) for $p := [k_p \; k_v]$. We will consider two different cases for two different amounts of time-delay in the feedback loop.

Case A-1: As shown in Fig. 1, the system (8) with (9) becomes unstable when h is greater than 0.085s. Therefore, we aim to design a controller for $h = 0.1$. Furthermore, we let (9) be the initial parameters for the optimization algorithm. As illustrated in Figs. 7 and 8, the controller with gains

$$k_p = 2.8701 [\frac{V}{rad}] \qquad k_v = 0.1010 [\frac{V \times s}{rad}] \,, \tag{20}$$

is designed after 39 iterations. The final spectral abscissa is determined as $c = -15.4471$. Furthermore, the optimal spectra is characterized by three modes as shown in Fig. 9. As a reference shaft angle, we use a square wave with certain

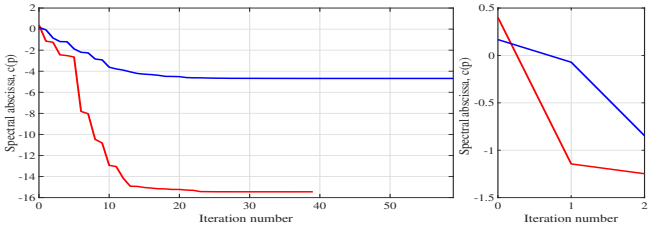

Fig. 8. Evolution of spectral abscissa during the course of the optimization process. The red line is for case A-1; the blue line is for case A-2.

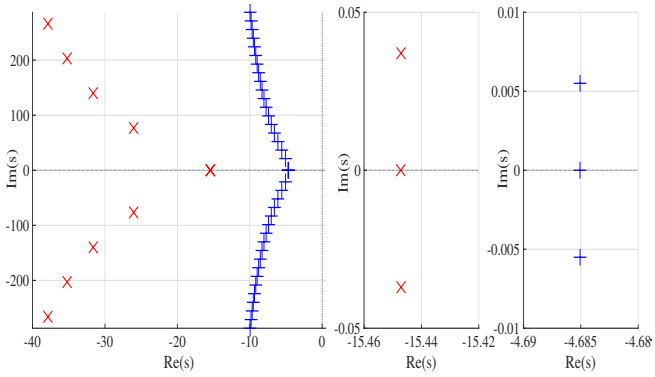

Fig. 9. -40-modes of (8) with the controller given in case A-1 (red "x") and the controller given in case A-2 (blue "+").

amplitude and frequency. As shown in Fig. 10 and Fig. 11, both simulated and measured response of the angular position is sufficiently fast and well-damped. We also investigate the delay margin of (8) with the designed controller. As shown in Fig. 12, the closed-loop system becomes unstable when h is about 0.35s. Therefore the delay margin is determined as about 0.25s.

Case A-2: Now, we will consider even a longer delay in the feedback loop. Considering that the controller in the previous case can stabilize the system only for delays up to 0.35s, we let $h = 0.4$. We choose the initial parameters for the optimization as in (20). As illustrated in Figs. 7 and 8, the controller with gains

$$k_p = 0.83281[\frac{V}{rad}] \qquad k_v = 0.0893[\frac{V \times s}{rad}], \tag{21}$$

is designed after 59 iterations. The final spectral abscissa is determined as $c = -4.6841$. As in Case A-1, the optimal spectra is characterized by three modes as shown in Fig. 9. Although the response of the angular position is slower than in Case A-1 (as it is expected), the response is still well-damped, as shown in Fig. 10 and Fig. 11. As shown in Fig. 12, the designed controller can stabilize the system for a time-delay of up to 1.3s, which gives a delay margin of about 0.9s, which is far better than the one achieved in the previous case.

We should note that, even though the designed controllers produce a satisfactory transient response, there exist a significant amount of steady state error, as shown in Fig. 11, in the experimental results. The error is especially high in case A-2, where the controller gains, given by (21), are relatively small. This result, which is also seen in many other works

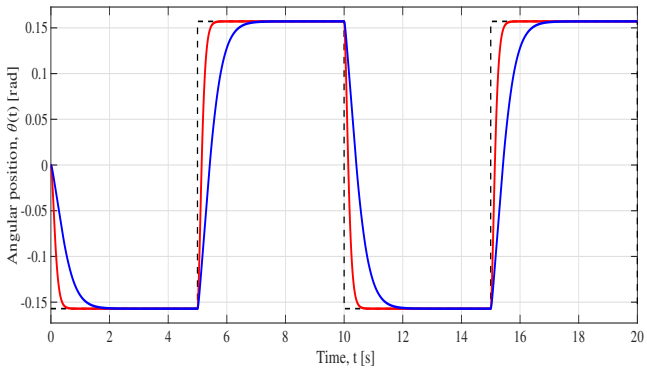

Fig. 10. Simulated response of the angular position with the gains given in case A-1 (red line), when $h = 0.1s$, and the gains given in case A-2 (blue line) when $h = 0.4s$. Dashed black lines indicate the reference.

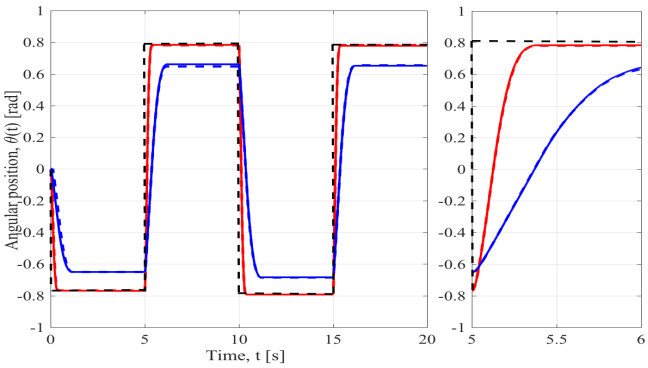

Fig. 11. Measured response of the angular position with the gains given in case A-1 (red line), when $h = 0.1s$, and the gains given in case A-2 (blue line) when $h = 0.4s$. Straight and dashed lines correspond to the case in which, respectively, encoder (with high-pass filter) and tachometer output is used to obtain angular speed. Dashed black lines indicate the reference.

(e.g., [9]), is mainly due to unmodeled friction effect. In order to reduce this error, one can add an integral action to PV controller, thus, design a PIV controller. A PIV controller can be designed by following exactly the same procedure by adding a third controller parameter, the integral gain.

B. Speed Control ($h \neq 0$)

In order to design a controller for (14), we will solve (16) for $p := [k_p \; k_i]$. As in the postion control, we will consider two different cases for two different amounts of time-delay in the feedback loop.

Case B-1: As shown in Fig. 4, the system (14) with (15) becomes unstable when h is greater than $0.012s$. Therefore, we aim to design a controller for $h = 0.02s$. Furthermore,

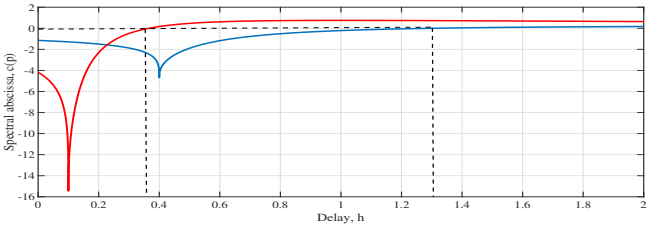

Fig. 12. Spectral abscissa of (8) with the controller given in case A-1 (red line) and the controller given in case A-2 (blue line) for changing values of delay.

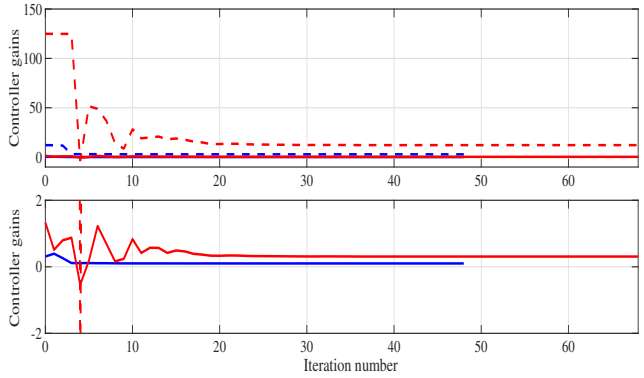

Fig. 13. Tunning of controller gains during the course of the optimization process. The straight lines are for k_p values; the dashed lines are for k_i values. Red color is used for case B-1; blue color is used for case B-2.

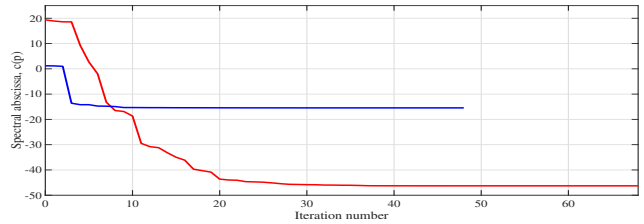

Fig. 14. Evolution of spectral abscissa during the course of the optimization process. The red line is for case B-1; the blue line is for case B-2.

we let (15) be the initial parameters for the optimization algorithm.

As illustrated in Figs. 13 and 14, the controller with gains

$$k_p = 0.3081[\frac{V}{rad/s}] \qquad k_i = 12.155[\frac{V}{rad}]\,, \tag{22}$$

is designed after 68 iterations. The final spectral abscissa is determined as $c = -46.2982$. Furthermore, the optimal spectra is characterized by three modes as shown in Fig. 15. As shown in Fig. 16 and Fig. 17, both simulated and measured response of the angular position is sufficiently fast and well-damped. Then, we investigate the delay margin of (14) with the designed controller. As shown in Fig. 18, the closed-loop system becomes unstable when h is about 0.085. Therefore the delay margin is determined as about $0.065s$.

Case B-2: In the previous case, the closed-loop system becomes unstable when the time-delay is above 0.085s.

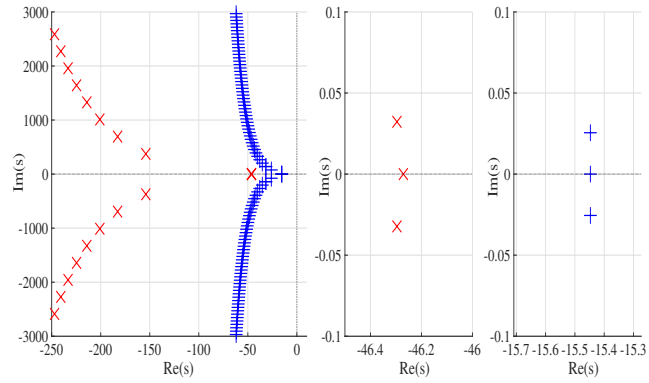

Fig. 15. -250-modes of (14) with the controller given in case B-1 (red "x") and the controller given in case B-2 (blue "+").

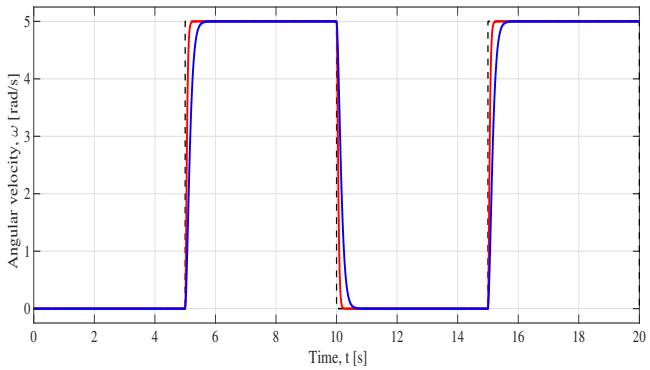

Fig. 16. Simulated response of the angular speed with the gains given in case B-1 (red line), when $h = 0.02s$, and the gains given in case B-2 (blue line) when $h = 0.1s$. Dashed black lines indicate the reference.

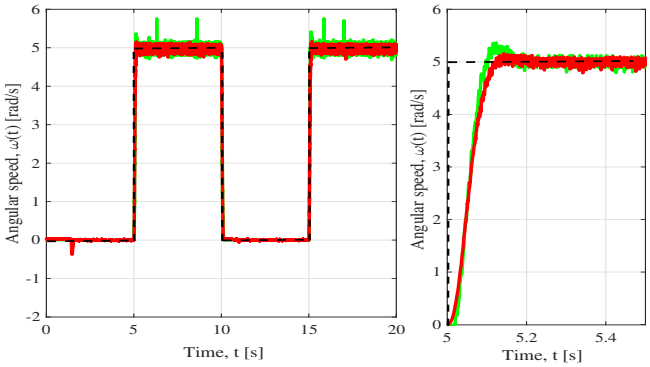

Fig. 17. Measured response of the angular speed with the gains given in case B-1 when $h = 0.02s$. Red lines corresponds to encoder (with high-pass filter) output, and green lines corresponds to tachometer output. Dashed black lines indicate the reference.

Regarding that, we aim to design a controller for $h = 0.1$ by letting the initial parameters be the gains given by (22).

As illustrated in Figs. 13 and 14, the controller with gains

$$k_p = 0.101[\frac{V}{rad/s}] \qquad k_i = 2.87[\frac{V}{rad}]\,, \tag{23}$$

is designed after 48 iterations. The final spectral abscissa is determined as $c = -15.4471$. As in Case B-1, the optimal spectra is characterized by three modes as shown in Fig. 15. Although the response of the angular position is slower than in Case B-1 (as it is expected), the response is still well-damped, as shown in Fig. 16 and Fig. 19. This controller can stabilize the system for a time-delay of up to $h = 0.365s$, as shown Fig. 18.

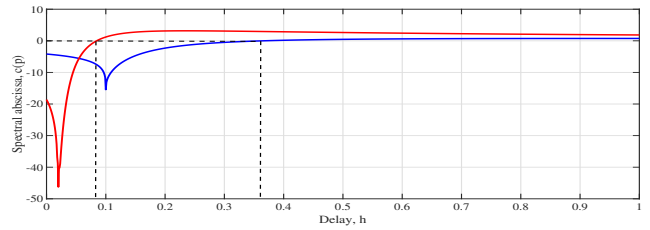

Fig. 18. Spectral abscissa of (14) with the controller given in case B-1 (red line) and the controller given in case B-2 (blue line) for changing values of delay.

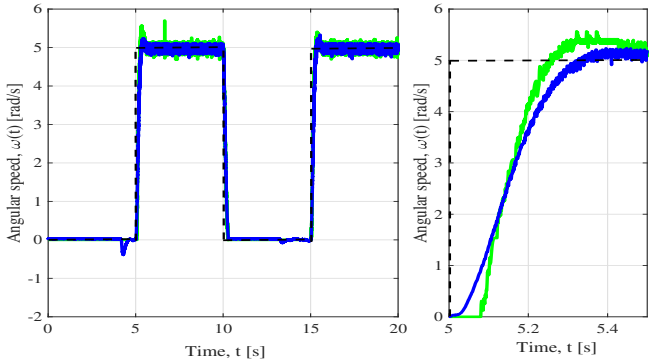

Fig. 19. Measured response of the angular speed with the gains given in case B-2 when $h = 0.1s$. Blue lines correspond to encoder (with high-pass filter) output, and green lines correspond to tachometer output. Dashed black lines indicate the reference.

V. Concluding Remarks

A nonsmooth optimization based stabilization method has been used to design PV and PI controllers for a DC-motor system with a pointwise time-delay in the feedback loop. Both simulations and experimental results show that the time-domain response is satisfactory. Furthermore, a significant amount of delay margin is also achieved.

We should note that the spectral abscissa is a non-convex function of controller parameters, in general. Thus, a proper initialization is crucial for the optimization problem (16) [25]. In this study, we initialize the controller parameters as those which give desired mode locations for the delay-free case and obtained satisfactory results. In general, however, (16) may be solved for multiple randomly chosen initial parameters in order to obtain different solutions from which the best one can be chosen.

By solving (16), one actually tries to minimize the real part of the rightmost modes. This, in turn, results in as fast a response as possible. The imaginary part of the modes, thus, are not controlled. In some applications, however, the imaginary parts of the dominant modes may be important, in order to meet certain time-domain specifications. In such a case, the optimization based controller design process can be followed by the *continuous pole placement* algorithm of [26] which allows to control both real and imaginary parts of a mode by tunning the controller parameters.

Although our present results show that the controllers designed by the present approach can achieve significant delay margins, we have not employed any mechanism to guarantee any robustness margins. Therefore, as a future study, robustness constraints can be added to the present optimization problem in order to guarantee desired robustness against time-delays and/or other uncertainties in the plant model.

References

[1] Q. G. Wang, Z. Zhang, K. J. Astrom, and L. S. Chek, "Guaranteed dominant pole placement with PID controllers," *Journal of Process Control*, vol. 19, no. 2, pp. 349–352, 2009.

[2] R. Sipahi, S.-I. Niculescu, C. Abdallah, W. Michiels, and K. Gu, "Stability and stabilization of systems with time delay," *IEEE Control Systems Magazine*, vol. 31, no. 1, pp. 38–65, 2011.

[3] W. Michiels and S.-I. Niculescu, *Stability, Control, and Computation for Time-Delay Systems: An Eigenvalue-Based Approach*. Philadelphia: SIAM, 2014.

[4] O. J. M. Smith, "A controller to overcome dead time," *Instrument Society of America Journal*, vol. 6, pp. 28–33, 1959.

[5] S. Majhi and D. P. Atherton, "Modified Smith predictor and controller for processes with time delay," *IEE Proceedings - Control Theory and Applications*, vol. 146, pp. 359–366, 1999.

[6] G. Meinsma and H. Zwart, "On $\mathscr{H}_\infty$ control for dead-time systems," *IEEE Transactions on Automatic Control*, vol. 45, pp. 272–285, 2000.

[7] O. Toker and H. Özbay, "On the rational $\mathscr{H}^\infty$ controller design for infinite dimensional plants," *International Journal of Robust and Nonlinear Control*, vol. 6, pp. 383–397, 1996.

[8] V. Kolmanovskii, S.-I. Niculescu, and J. P. Richard, "On the Liapunov-Krasovskii functionals for stability analysis of linear delay systems," *International Journal of Control*, vol. 72, pp. 374–384, 1999.

[9] S. Yi, P. W. Nelson, and A. G. Ulsoy, "DC motor control using the Lambert W function approach," in *Proceedings of the 10th IFAC Workshop on Time Delay Systems*, Boston, MA, U.S.A., Jun. 2012.

[10] ——, "Proportional-integral control of first-order time-delay systems via eigenvalue assignment," *IEEE Transactions on Control Systems Technology*, vol. 21, pp. 1586–1594, 2013.

[11] J. Vanbiervliet, K. Verheyden, W. Michiels, and S. Vandewalle, "A nonsmooth optimisation approach for the stabilisation of time-delay systems," *ESAIM: Control, Optimisation and Calculus of Variations*, vol. 14, no. 3, pp. 478–493, 2008.

[12] S. Gümüşsoy and W. Michiels, "Fixed-order H-infinity control for interconnected systems using delay differential algebraic equations," *SIAM Journal on Control and Optimization*, vol. 49, pp. 2212–2238, 2011.

[13] W. Michiels, T. Vyhlidal, and P. Zitek, "Control design for time-delay systems based on quasi-direct pole placement," *Journal of Process Control*, vol. 27, pp. 337–343, 2010.

[14] D. Pilbauer, T. Vyhlidal, and W. Michiels, "Spectral design of output feedback controllers for systems pre-compensated by input shapers," in *Preprints of the 12th IFAC Workshop on Time-delay Systems*, Ann Arbor, MI, USA, Jun. 2015.

[15] S. M. Özer and A. İftar, "Controller design for neutral time-delay systems by nonsmooth optimization," in *Preprints of the 13th IFAC Workshop on Time-delay Systems*, Istanbul, Turkey, Jun. 2016, pp. 212–217.

[16] S. M. Özer, G. Gülmez, and A. İftar, "A software to design decentralized controllers for time-delay systems," in *Proceedings of the 2016 IEEE Conference on Computer Aided Control System Design*, Buenos Aires, Argentina, Sep. 2016, pp. 868–873.

[17] J. K. Hale and S. M. Verduyn-Lunel, *Introduction to Functional Differential Equations*. New York: Springer-Verlag, 1993.

[18] Z. Wu and W. Michiels, "Reliably computing all characteristic roots of delay differential equations in a given right half plane using a spectral method," *Journal of Computational and Applied Mathematics*, vol. 236, pp. 2499–2514, 2012.

[19] Quanser, *SRV-02 Rotary Servo Based Unit User Manuel*. Canada: QUANSER, 2015.

[20] J. V. Burke, A. S. Lewis, and M. L. Overton, "A robust gradient sampling algorithm for nonsmooth, nonconvex optimization," *SIAM Journal on Optimization*, vol. 15, pp. 751–779, 2005.

[21] A. S. Lewis and M. L. Overton, "Nonsmooth optimization via quasi-Newton methods," *Mathematical Programming*, vol. 141, no. 1, pp. 135–163, 2012.

[22] M. Overton, "HANSO: A hybrid algorithm for nonsmooth optimization," Tech. Rep., 2009, http://cs.nyu.edu/overton/software/hanso.

[23] H. E. Erol and A. İftar, "Decentralized controller design by continuous pole placement for neutral time-delay systems," *Transactions of the Institute of Measurement and Control*, vol. 39, pp. 297–311, 2017.

[24] J.-P. Richard, "Time-delay systems: an overview of some recent advances and open problems," *Automatica*, vol. 39, pp. 1667–1694, 2003.

[25] S. M. Özer and A. İftar, "Decentralized controller design for time-delay systems by optimization," in *Preprints of the 12th IFAC Workshop on Time-delay Systems*, Ann Arbor, MI, USA, Jun. 2015, pp. 462–467.

[26] W. Michiels, K. Engelborghs, P. Vansevenant, and D. Roose, "Continuous pole placement for delay equations," *Automatica*, vol. 38, pp. 747–761, 2002.